



ELSEVIER

Journal of Chromatography A, 779 (1997) 185–194

JOURNAL OF
CHROMATOGRAPHY A

Ultrasensitive near-infrared laser-induced fluorescence detection in capillary electrophoresis using a diode laser and avalanche photodiode

Benjamin L. Legendre Jr., Dixie L. Moberg, Daryl C. Williams, Steven A. Soper*

Department of Chemistry, Louisiana State University, Baton Rouge, LA 70803-1804, USA

Received 15 January 1997; received in revised form 4 March 1997; accepted 7 April 1997

Abstract

A sensitive fluorescence detector for capillary electrophoresis consisting of a semiconductor near-infrared diode laser and a single photon avalanche diode (SPAD) is described. The sensitivity of this system was demonstrated by the separation and analysis of four tricarboyanine dyes using capillary electrophoresis and a running buffer consisting of 98% methanol and 2% water with 40 mM borate (pH 9.4). The LOD for the dye, IR-132, was found to be 4.41 zmol with the dynamic range found to be approximately four orders of magnitude in concentration. Based on the sampling volume of the system, the number of molecules actually detected at this LOD was approximately 27. To further demonstrate the utility of this diode-based detector, various amino acids were derivatized with a highly anionic near-IR labelling dye. The conjugates were separated in a running buffer comprised of predominately methanol and a cationic surfactant added to reverse the electroosmotic flow. The LOD values for various amino acids were found to be in the low zmol range. © 1997 Elsevier Science B.V.

Keywords: Amino acids; Laser-induced fluorescence detection; Near-infrared diode laser; Single-photon avalanche diode; Detection, electrophoresis

1. Introduction

Capillary electrophoresis (CE) coupled to laser-induced fluorescence (LIF) detection has become an important analytical tool due to the impressive detection limits, fast analysis times, high separation efficiencies and the ability to use small sample volumes. The common lasers used for excitation in these applications are the gas-ion lasers, such as the He–Cd, Ar ion or He–Ne lasers. As a consequence of the use of these lasers, the common approach has

been to implement detection in the visible region of the electromagnetic spectrum due to the wide choice in labelling dyes that match common lasing lines of these gas ion lasers. Dovichi et al. has demonstrated LIF detection in the subattomole range for various fluorescein isothiocyanate (FITC) derivatives of the amino acids using an argon ion laser for excitation in the visible region and the detection performed off-column in a sheath-flow cuvette arrangement [1].

Incorporation of a diode laser for LIF detection can potentially provide many advantages over conventional laser-based excitation sources. The principle advantages associated with diode lasers include;

*Corresponding author.

inexpensive, compact, long operational lifetimes (>40 000 h), stable output and relatively high powers in the near-infrared (near-IR) [2]. In addition, diode lasers are conducive to miniaturization and can potentially be run using a simple DC battery.

Mank and Yeung have recently demonstrated the use of a far-red laser-induced fluorescence detector in capillary electrophoresis [3]. Using a dicarbocyanine label ($\lambda_{\text{abs}}=667$ nm), they were able to achieve a mass detection limit of 0.1 amol for various primary amines. In this work, a diode laser with a lasing line at 670 nm was used as the excitation source and the photon transducer consisted of a red-sensitive photomultiplier tube. Chen et al. also reported on a far-red diode-based laser-induced fluorescence detector for capillary electrophoresis [4]. In this work, Cy5 ($\lambda_{\text{abs}}=670$ nm) was used to label a DNA sequencing primer and the conjugate was separated in a capillary gel column. They reported a concentration detection limit of 10^{-10} M for this dye-labelled primer.

The near-IR (750–1000 nm) can potentially offer improved performance in capillary electrophoresis compared to the far-red due to the fact that fluorescence impurities, especially when dealing with complex biological samples, can be substantially lower in the near-IR. In addition, the fluorescence observation windows, free from Raman scattering, can be substantially larger in the near-IR due to the lower energy of the excitation photons and the fact that the Raman cross-sections scale to $1/\lambda^4$. Also, many diode lasers can be operated at higher lasing powers (780–830 nm) than the far-red diode lasers, improving the signal-to-noise ratio in a fluorescence measurement.

Near-IR fluorescence has already been demonstrated to provide a viable alternative to visible fluorescence analyses in many bioanalytical applications [5–11]. The dyes typically used in the near-IR are the tricarbocyanines which possess heteroaromatic fragments linked by a heptamethine chain. The major difficulties associated with the use of these near-IR fluorophores are the poor photophysical properties they show in aqueous solvents and the lack of sufficient labels for the tagging of various compounds [12–16]. In pure aqueous solvents, many of these dyes show extensive ground-state aggregation, fluorescence quantum yields

<0.10 and photochemical stabilities inferior to most visible dyes. Modifications in the molecular structure, however, can improve these fluorescence properties. For example, the addition of alkyl sulfonate groups to the dye can improve the water solubility as well as the quantum yield and photochemical stability [17]. To alleviate the problem of poor photophysical properties associated with these chromophores in water, the addition of organized media, such as surfactants used above their critical micelle concentration, into the aqueous solvent or the use of organic modifiers in the solvent can improve the analytical performance [18–21].

In the case of CE, differences in the separation parameters that arise from the use of organic modifiers in the running buffer include changes in the electroosmotic flow, reduced Joule heating due to the lower current and enhanced resolution [22–25]. Moreover, nonaqueous or mixed organic/aqueous running buffers can be useful for the electrophoretic separation of solutes that have poor solubilities in water. We have recently shown that in predominantly aqueous buffers, the efficiency for the CE separation of a series of cationic tricarbocyanine dyes was very poor [26]. Adding methanol to the buffer significantly improved the efficiency due to the minimization of solute-wall interactions. Using an Ar ion pumped Ti:sapphire laser and an avalanche photodiode, we were able to achieve a molecular detection limit of 429 molecules for IR-132 in a running buffer consisting of methanol–water (95:5, v/v) (pH 9.0). In this work, we wish to report on the use of a diode-based near-IR laser-induced fluorescence detection system for the analysis of native near-IR dyes and near-IR dye-labelled amino acids separated by CE in different methanol–water running buffers with detection performed on-column. The near-IR LIF detector consisted of a GaAlAs diode laser and a single photon avalanche diode (SPAD). The diode laser (10 mW, 785 nm) produced a circular output beam by incorporating an intracavity anamorphic prism pair which provided easy focusing onto the capillary. The photon transducer was a SPAD, which has a large single-photon detection efficiency in the near-IR. We carried out CE experiments on four commercially available dyes to produce a calibration plot in order to show the limits of detection for this system along with the detector dynamic range. Also,

amino acids were labelled with a highly anionic isothiocyanate near-IR dye and separated using CE with mixed organic/aqueous running buffers containing cationic surfactants to reverse the direction of the electroosmotic flow.

2. Experimental

2.1. Diode-based LIF detector

A block diagram of the diode-based near-IR LIF detector is shown in Fig. 1. The excitation source was a GaAlAs diode laser (Melles Griot, model 06 DLD 201), equipped with an intracavity anamorphic prism pair in order to produce a circular output beam in a pseudo-Gaussian TE mode structure to allow tight focusing [beam waist ($1/e^2$) = 7 μm]. The laser was tuned to 785 nm ($T=25^\circ\text{C}$) and delivered 10 mW of laser light to the capillary. The temperature of the diode head was controlled with a thermoelectric cooler in order to prevent mode-hopping arising from temperature drifts. The fluorescence emission was collected in a conventional 90° format with a $60\times$ high numerical aperture microscope objective

(Nikon, Natick, MA, USA; NA=0.85). The emission was spatially filtered with a 0.4 mm slit, producing a viewing distance of 6.7 μm along the propagation axis of the laser. The fluorescence was further isolated from the scattering photons with an eight cavity interference filter (CWL 850 nm, HBW 30 nm, Omega Optical, Brattleborough, VT, USA). The fluorescence emission was focused onto the photodetector by a $10\times$ microscope objective (Melles Griot), producing an image of approximately 20 μm on the face of the detector. The photodetector was a single-photon avalanche diode (SPAD, EG and G Electrooptics Canada, Vandreuil, Canada) mounted on a thermoelectric cooler with a photoactive area of 1.77×10^{-4} cm^2 (I.D.=150 μm) and possessed a dark count rate of approximately 50 cps. The pulses from the SPAD were amplified and conditioned using a discriminator (Tennelec TC 754, Oak Ridge, TN, USA) with the output from the discriminator sent to a multichannel scaler resident in a PC486 for displaying the electropherograms (Tennelec PCA II).

2.2. Capillary electrophoresis (CE)

The CE columns were initially rinsed with 0.15 M NaOH for 1 h followed by a 2 h wash with water. Prior to the electrophoresis, the capillary was allowed to equilibrate with the appropriate running buffer for 30 min under high voltage conditions (400 V/cm). The high voltage power supply was obtained from Spellman High Voltage Electronics Corp. (CZ1000R, Plainview, NY, USA). All separations were carried out at ambient temperatures (25°C). The capillary column (Polymicro, Phoenix, AZ, USA) used for the separations was a 75 μm I.D. tube cut to a total length of 62 cm (55 cm to detection window). The detection window was made using an electrically heated resistor to remove the polyimide coating.

2.3. Reagents

The cationic near-IR dyes DTTCl, HITCl, IR-140 and IR-132 were purchased from Kodak Chemical (Rochester, NY, USA) and used as received (see Fig. 2 for structures). Spectroscopic grade methanol was received from Mallinckrodt Chemical (Paris, NY, USA). The near-IR dye solutions for CE analysis were prepared daily in the running buffer (98:2

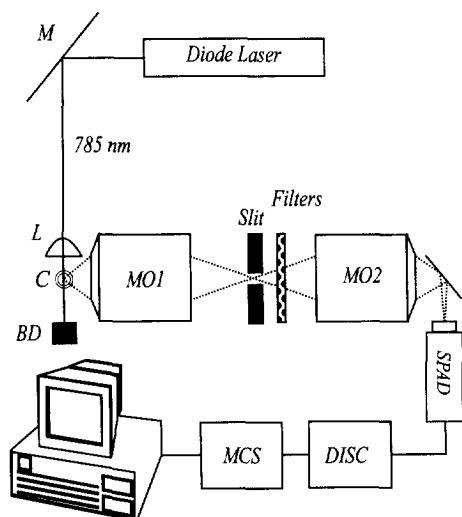


Fig. 1. Block diagram of the diode-based near-IR LIF detection system. M=mirror; L=laser focusing lens; C=capillary; BD=beam dump; MO1=collection microscope objective; MO2=focusing microscope objective; SPAD=single photon avalanche diode; DISC=discriminator; MCS=multichannel scaler.

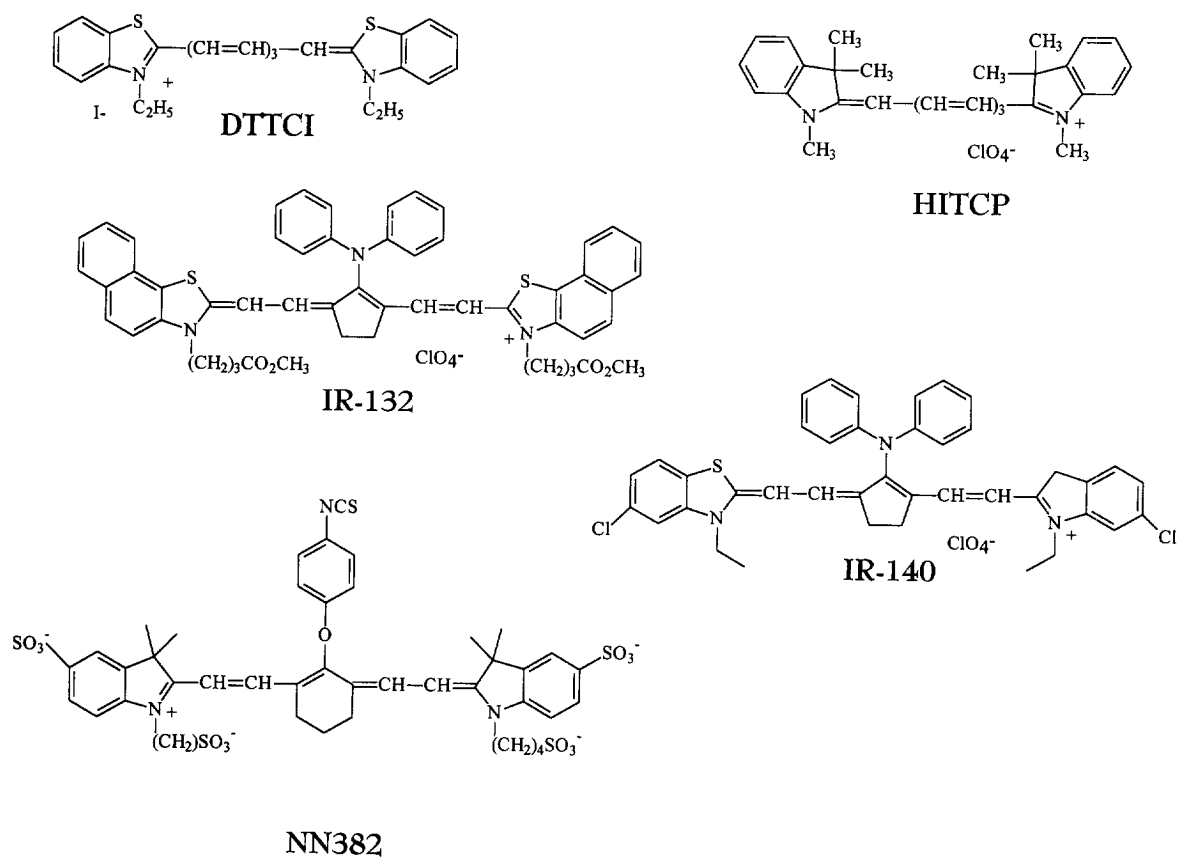


Fig. 2. Chemical structures of the near-IR labelling dye, NN382 and the cationic dyes, IR-132, DTTCl, IR-140 and HITCP.

methanol–water, 40 mM borate, pH 9.4) from a serial dilution of a 1×10^{-6} M standard solution of the dyes stored at 10°C in methanol. The near-IR labelling dye (NN382) used for the LIF detection of primary amines was obtained from Li-Cor (Lincoln, NE, USA) and contained an isothiocyanate functional group (see Fig. 2) for covalent attachment of the dye to the primary amine. Cetyltrimethylammonium bromide (CTAB, CMC=0.9 mM) and the amino acids were purchased from Sigma Chemical.

2.4. Conjugation of near-IR chromophore to amino acids

A 1×10^{-2} M stock solution of NN382 was prepared in dimethylformamide (Aldrich Chemical,

Milwaukee, WI, USA) and a 5×10^{-4} M solution of each amino acid was prepared in 40 mM borate (pH 9.4). The labelling reaction was carried out at a pH 9.4 in borate (40 mM) and enough dye was added to produce an approximate three-fold molar excess of the near-IR labelling dye. All derivatization reactions of the single amino acids were carried out at a concentration of 5 μ M and, in the case of the multiple amino acid analysis, the total amine concentration was set to 5 μ M. The amino acid/NN382 solutions were allowed to conjugate in the dark at room temperature with constant agitation for 12–16 h. The derivatization mixtures were then serially diluted to the appropriate concentration in the electrophoresis running buffer and electrokinetically injected onto the capillary column.

3. Results and discussion

3.1. Detection limits of native near-IR dyes

To determine the sensitivity and LOD values of the diode-based LIF detector, a series of CE separations of some model cationic near-IR dyes (DTTCl, HITCl, IR-140 and IR-132) were performed over a concentration range of 10^{-10} to 10^{-13} M. In Fig. 3A is shown the electropherogram of these dyes at an injection concentration of 2.0×10^{-12} M. The running buffer used in this case consisted of 98:2 methanol–water which was buffered using borate at an apparent pH of 9.4. The need for this high methanol content in the running buffer results from the fact that these dyes show improved photophysics in predominately methanol solvents [16]. In addition, these cationic polymethine dyes demonstrate severe solute-wall interactions, significantly deteriorating CE efficiency in high aqueous content running buffers, with the addition of methanol improving both CE efficiency and detectability [26]. At this dye concentration and injection conditions, the mass of dye contained in each peak shown in Fig. 3A corresponds to approximately 20 zmol ($V_{inj} \approx 10$ nl).

In Fig. 3B is shown a calibration plot constructed for these dyes over this concentration range. Each point in the plot represents the average of three replicate measurements, with the standard deviations shown as the error bars. The correlation coefficient yielded values >0.99 , indicating that the response of the detector is linear over this particular concentration range (4 orders of magnitude). The calibration plot could be extended by another order of magnitude (10^{-9} M, data not shown), but it was found the correlation coefficients decreased dramatically. The upper limit in linearity is determined primarily by saturation of the SPAD. The current SPAD is operated in a passive quenching mode of the avalanche process, and as such, can accept counting rates (before saturation) of approximately 500 000 cps. However, the dynamic range could be increased by using a SPAD with an active quenching circuit, which can process counts at rates exceeding 2–4 million cps.

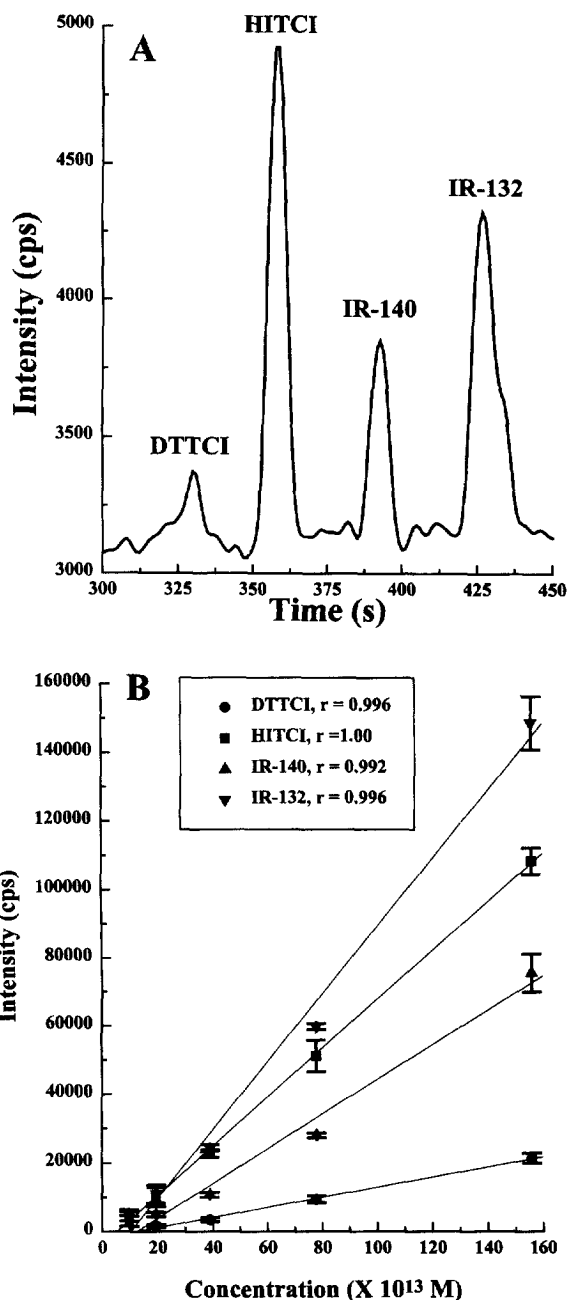


Fig. 3. Electropherogram of four near-IR dyes at 2.0×10^{-12} M (A) and a calibration plot of these dyes over the concentration range of 10^{-10} to 10^{-13} M (B). The electrophoresis conditions were as follows; $V_{inj} = 25$ kV; $t_{inj} = 5$ s; $E_{sep} = 400$ V/cm; $L_{tot} = 62$ cm; capillary I.D. = 75 μ m; laser power = 10 mW. The running buffer consisted of 98:2 methanol–water and was buffered at pH 9.4 using borate (40 mM).

The on-column mass detection limits (SNR=3) for these near-IR dyes, DTTCl, HITCl, IR140 and IR-132 were found to be 22.1, 4.79, 7.20 and 4.41 zmol, respectively. The higher detection limit for DTTCl resulted from the poorer photochemical stability associated with this dye. In our previous work on the electrophoretic separation of these dyes using a 95:5 methanol–water running buffer and a Ti:sapphire laser for excitation, the on-column mass detection limit for IR-132 was found to be 0.43 zmol. Therefore, the on-column mass LOD using the less expensive diode laser was found to be only a factor of 10 poorer than those achieved using the more sophisticated Ti:sapphire laser-based system. Based on the slit width of the detection system, the diameter of the laser beam and the capillary I.D., only approximately 1% of the molecules migrating through the capillary column are effectively sampled. Therefore, the number of molecules that actually produce the observed signals at these LODs are 133, 28, 44 and 27 for DTTCl, HITCl, IR-140 and IR-132, respectively. The molecular detection limits for these fluorescent dyes separated using CE are comparable to those reported by Dovichi and coworkers, who detected single phycoerythrin molecules, which are effectively equivalent to 22 R6G molecules, in CE excited by visible excitation from an Ar ion laser and off-column detection in a sheath flow cell [27].

3.2. CE of NN382

In order to separate a series of amino acids using CE with NIR–LIF detection, the labelling dye, NN382 (see Fig. 2), was used. This dye contains multiple alkyl sulfonate groups that not only improves water solubility, but can also enhance photochemical stability [17]. In addition, the dye has an absorption maximum at 787 nm in methanol, nicely matching the lasing line of the GaAlAs diode laser.

The electropherograms of NN382 in various methanol–water running buffers are shown in Fig. 4A. In general, as the amount of methanol was increased in the running buffer, the LIF signal increases, most likely resulting from enhancement in the photophysical properties of the dye in organic solvents. Also, the efficiency of the separation is strongly influenced by the percentage of methanol in the running buffer. From Fig. 4A, the plate numbers

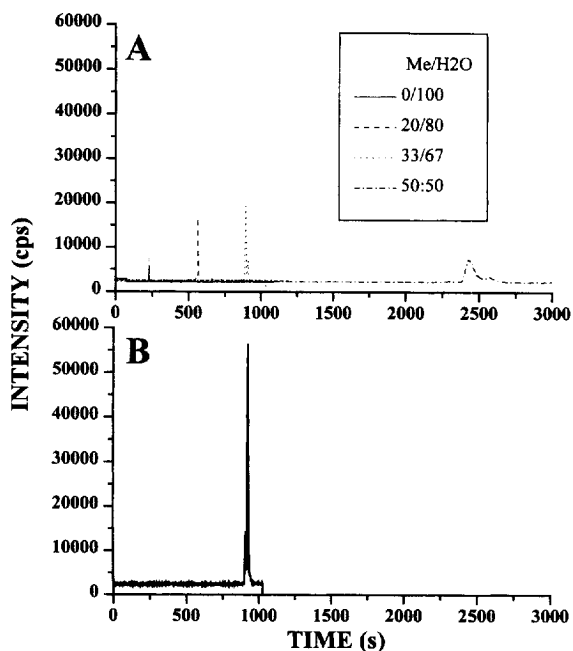


Fig. 4. Electropherograms of 1×10^{-10} M NN382 in various methanol–water concentrations ranging from 0 to 50% methanol with 40 mM borate, pH 9.4 run in positive polarity (A) and in 50:50 water–methanol, 0.55 mM CTAB, 40 mM borate, pH 9.4 using reverse polarity (B). The electrokinetic injection times were varied in order to insert the same amount of material onto the column in all cases. All other electrophoretic conditions were the same as those in Fig. 3.

(per meter) in a 0:100 methanol–water buffer was calculated to be $107\,000\text{ m}^{-1}$ and increased to $123\,000\text{ m}^{-1}$ for the 20:80 methanol–water buffer. When the methanol content was increased to 33%, the efficiency dropped to $117\,000\text{ m}^{-1}$, most likely due to increased residence time on the column resulting in increased zone broadening from longitudinal diffusion. In addition, the presence of a second peak (impurity) was resolved from the major dye peak in the 33:67 methanol–water buffer, which comigrated at lower methanol compositions. When the methanol content was increased to 50%, the number of theoretical plates decreased dramatically to $12\,300\text{ m}^{-1}$, resulting from its low apparent mobility produced from the reduced electroosmotic flow at high methanol contents [28], giving significant zone broadening due to longitudinal diffusion.

Also apparent from Fig. 4A is that the net fluorescence signal for NN382 increases as the

methanol composition is increased. For example, the integrated area under the NN382 peak (background corrected) was found to be 9300 counts when no methanol was present in the running buffer and increased to over 78 500 counts when the running buffer contained 33% methanol, nearly an eight-fold increase in signal.

In order to circumvent the problem of poor efficiency resulting from excessively long migration times associated with high methanol content running buffers, a cationic surfactant, such as CTAB below its critical micelle concentration, was added to the 50:50 methanol–water CE buffer (40 mM borate, pH 9.4) and reversing the polarity of the CE system. The results of these changes are shown in Fig. 4B for NN382. In this case, the efficiency was found to be $130\,000\text{ m}^{-1}$ and the migration time was 926 s, compared to 2550 s when the CE was performed in positive polarity with the same methanol composition in the running buffer. Integrating the area under the peak shown in Fig. 4B produced a net signal of 449 000 counts, a 50-fold improvement in signal strength compared to the case when no methanol was present in the running buffer. In addition, it was found that no significant increases in the background were observed when surfactants in high methanol concentration running buffers were used. For the 100% water running buffer, the magnitude of the background was 2500 cps, while for the 50:50 methanol–water buffer with CTAB, the background under similar operating conditions was only 2700

cps. This result is a direct consequence of the use of near-IR excitation and detection and the fact that few compounds show intrinsic fluorescence in this region of the electromagnetic spectrum. The SNR for NN382 using the 0:100 methanol–water buffer was found to be 106, while in the case of 50:50 methanol with CTAB and run in reverse polarity, the SNR for the same injected mass of NN382 was found to be 2320.

3.3. Separation and detection of near-IR labelled amino acids

A series of amino acids were conjugated to NN382 individually and the conjugates analyzed using CE (reverse polarity) with a running buffer consisting of 50:50 methanol–water, 0.55 mM CTAB and 40 mM borate (pH 9.4) in order to investigate the labelling efficiencies, mobilities and detectabilities using near-IR diode LIF detection. The results of this investigation are summarized in Table 1. The neutral amino acids, such as tryptophan and phenylalanine, migrate first when conjugated to NN382, since these amino acid–dye complexes have an additional negative charge resulting from the carboxylate group on the amino acid. The near-IR labelling dye can potentially produce doubly-labelled conjugates to the amino acids lysine and arginine, due to the two primary amine groups. If NN382 were to label both primary amine groups of lysine and arginine, the amino acid–dye complex would have a

Table 1
Labelling efficiency, mobilities and detection limits for various NN382-labelled amino acids using CE with near-IR LIF detection

Amino acid	Migration time (s)	Conjugation efficiency (%)	Mobility ($\text{cm}^2/\text{V s}$, $\times 10^4$)	Plates (m^{-1} , $\times 10^{-5}$)	LOD (zmol, SNR=3)
SER	960	30.1	1.43	2.42	65.3
GLY	963	64.8	1.43	2.21	26.2
VAL	968	43.0	1.42	2.62	37.8
GLN	975	44.4	1.41	2.66	33.2
MET	976	58.4	1.41	4.53	21.2
LEU	981	48.7	1.40	5.50	27.5
PHE	982	81.0	1.40	3.59	16.5
TRP	990	62.3	1.39	4.47	20.2
LYS	1137	30.7	1.21	3.87	64.3
ARG	1148	78.9	1.20	2.87	27.1
HIS	1156	20.0	1.19	0.77	401

The CE was performed at a field strength of 400 V/cm and operated in a reverse polarity mode. The running buffer was 50:50 methanol–water, with 0.55 mM CTAB and buffered with borate (40 mM) at pH 9.4.

net charge of -7 at this pH, and should migrate much sooner than the free dye using reverse polarity. However, no peaks were observed early in the electropherogram arising from these amino acids indicating that double-labelling was not present to any significant amount. The preclusion of double labelling would be expected based solely on steric considerations due to the extended size of the labelling dye. The basic amino acids, histidine, lysine and arginine, were all found to migrate after the free dye.

The labelling efficiency of the dye to these specific amino acids is also shown in Table 1. For these amino acids, the labelling efficiency ranged from 20.0% for histidine to 81.0% for phenylalanine. The labelling efficiency was calculated by taking the net signal from the amino acid/NN382 peak and dividing it by the net signal produced from the NN382 peak in the blank CE run. It was also noted that the kinetics of the labelling were slow. Complete labelling was found to occur only after approximately 12 h of reaction time at room temperature. In addition, we attempted to label several different acidic amino

acids and found that the extent of labelling was minimal. We have attributed this observation to electrostatic considerations; the excess negative charge on the dye and the acidic amino acid at alkaline pHs decrease the probability of a bimolecular interaction.

The detection limits for these amino acids and the plate numbers are also shown in Table 1. The plate numbers ranged from $77\,300\text{ m}^{-1}$ for the histidine–dye conjugate to $550\,000\text{ m}^{-1}$ for the leucine–dye conjugate. The mass limit of detection for these amino acids were found to range from 16 zmol for phenylalanine to 401 zmol for histidine (see Table 1). The poorer LOD for histidine most likely resulted from the inefficient labelling as well as the broad peak produced in the CE analysis.

Fig. 5 shows an electropherogram for a mixture of six amino acid–NN382 dye complexes separated by CE in reverse polarity. These six amino acids were chosen due to differences in their mobilities under these CE conditions. As can be seen, adequate resolution was obtained in this case. The total development time of this electropherogram was

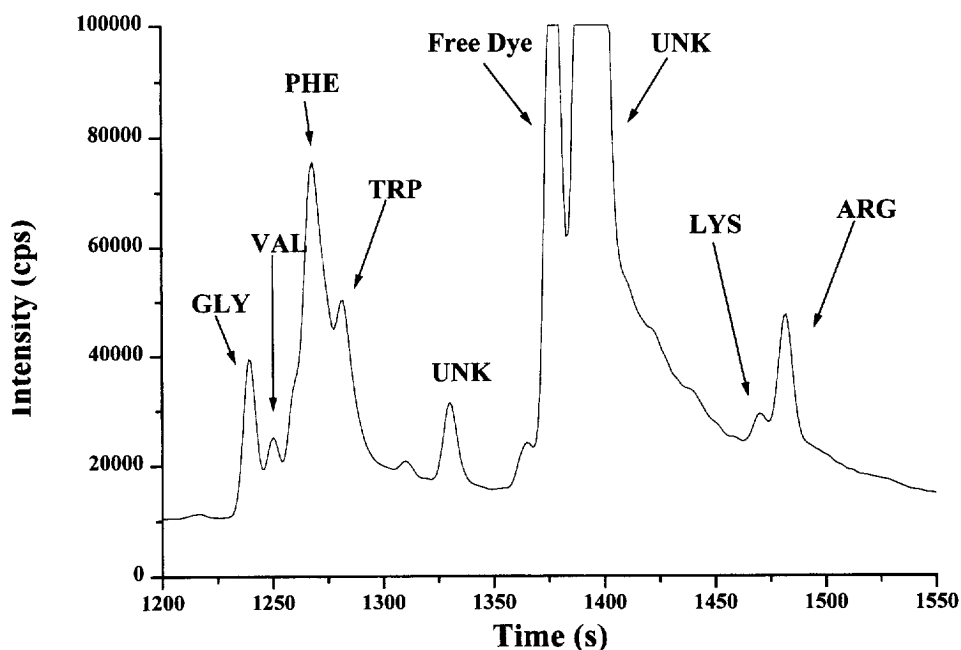


Fig. 5. Electropherogram of a mixture of six labelled amino acids with NN382 and detected using the diode-based, near-IR LIF detector. The running buffer consisted of 50:50 methanol–water, 0.55 mM CTAB, 40 mM borate, pH 9.4 with the system run in reverse polarity. The electrophoretic conditions were as follows: [amino acid] = 1.3×10^{-9} M; [NN382] = 4×10^{-8} M; V_{inj} = 10 kV; t_{inj} = 5 s; E_{sep} = 270 V/cm.

found to be 1500 s, which was obtained at a field strength of 270 V/cm. At higher field strengths, the resolution was found to be inadequate and further reductions in the field strength led to a loss in peak definitions and efficiency due to excessive longitudinal diffusion.

4. Conclusions

We have demonstrated the feasibility of using a diode laser as an excitation source for a near-IR fluorescence detector with a SPAD serving as the photodetector in CE applications. Incorporation of the diode laser provides a compact system which is simple to operate, durable and inexpensive. In addition, the use of near-IR excitation and detection is immune to background problems resulting from impurity fluorescence and scattering generated by the sample matrix. On-column detection limits for some model near-IR labelled amino acids were found to be comparable or better to those obtained using a more expensive Ar ion laser excitation source and off-column detection in a sheath flow cell. The use of near-IR fluorescence will be particularly advantageous when detection must be performed in a more complicated matrix, for example capillary gel electrophoretic analysis of oligonucleotides, where the gel matrix can produce a substantial background problem when using visible excitation and detection, degrading on-column detection limits.

However, improvements in labelling probes are still needed in order to make near-IR fluorescence a practical approach for the analysis of primary amines and other analytes, especially at low concentration levels. For example, we were unable to label any of the acidic amino acids using this anionic dye and the labelling efficiency for the basic and neutral amino acids was highly variable and never exceeded 90%. In addition, the labelling reaction was found to be quite slow. While the use of the highly anionic near-IR labelling dyes does show some advantages (water solubility, favorable photophysics), it also requires significant modifications in the CE operating conditions in order to optimize the analysis times and LOD values, for example, addition of large amounts of methanol into the running buffer and reversing the polarity of the CE system.

And finally, the ability to derivatize at low analyte concentrations is still a pervasive problem in the near-IR. Our derivatization reactions were carried out at an amine concentration of approximately 5 μM . Therefore, the detection limits reported herein represent those associated with the laser detector and not necessarily those associated with the labelling reactions. Attempts to derivatize these amines with NN382 at lower amino acid concentrations resulted in further reductions in the conjugation efficiency and slower kinetics. In addition, blank peaks, due to impurities in the dye or decomposition of the dye, were particularly evident. In order for near-IR fluorescence to become practical for low-level analysis of components in complex matrices, further improvements in labelling dyes appropriate for this region must be made.

Acknowledgments

The authors would like to thank the National Institutes of Health (R29-HG000A19) and the Louisiana Educational Quality Support Fund for financial support of this work. The authors would also like to thank Li-Cor Technologies (Lincoln NE) for the generous donation of the NN382 labelling dye used in these studies.

References

- [1] Y. Cheng, N.J. Dovichi, *Science* 242 (1988) 562–564.
- [2] T. Higashijima, T. Fuchigami, T. Imasaka, N. Ishibashi, *Anal. Chem.* 64 (1992) 711–714.
- [3] A.J.G. Mank, E.S. Yeung, *J. Chromatogr. A* 708 (1995) 309–321.
- [4] F.A. Chen, A. Tusak, S. Pentoney, K. Konrad, C. Lew, E. Koh, J. Sternberg, *J. Chromatogr.* 652 (1993) 355–360.
- [5] T. Imasaka, A. Yoshitake, *Anal. Chem.* 56 (1984) 1077–1079.
- [6] K. Sauda, T. Imasaka, N. Ishibashi, *Anal. Chim. Acta* 187 (1986) 353–356.
- [7] T. Imasaka, A. Tsudamoto, N. Ishibashi, *Anal. Chem.* 61 (1989) 2285–2288.
- [8] T. Imasaka, N. Ishibashi, *Anal. Chem.* 62 (1990) 363A–371A.
- [9] M.A. Roberson, D. Andrews-Wilberforce, D. Norris, G. Patonay, *Anal. Lett.* 23 (1990) 729–734.
- [10] G. Patonay, M. Antoine, S. Devanathan, L. Strekowski, *Appl. Spectrosc.* 45 (1991) 457–461.

- [11] M.A. Kessler, O.S. Wolfbeis, *Anal. Biochem.* 200 (1992) 254–259.
- [12] S.A. Soper, Q.L. Mattingly, P. Vegunta, *Anal. Chem.* 63 (1993) 740–747.
- [13] W. West, S.J. Pearce, *J. Phys. Chem.* 69 (1965) 1894–1903.
- [14] R.J. Williams, M. Lipowska, G. Patonay, *Anal. Chem.* 65 (1993) 601–605.
- [15] G. Patonay, M.D. Antoine, *Anal. Chem.* 63 (1991) 321A–327A.
- [16] S.A. Soper, Q.L. Mattingly, *JACS* 116 (1994) 3744–3752.
- [17] S. Soper, J. Huang, T. McCarley, *J. Fluoresc.*, 1996, submitted for publication.
- [18] R. Humphry-Baker, M. Gratzel, R. Steiger, *JACS* 102 (1980) 847–848.
- [19] H. Sato, M. Kawasaki, K. Kasatani, Y. Kusumoto, N. Nakashima, K. Yoshihara, *Chem. Lett.* 72 (1980) 1529–1532.
- [20] N. Nakashima, T. Kunitake, *JACS* 104 (1982) 4261–4262.
- [21] H. Sato, M. Kawasaki, K. Kasatani, Y. Kusumoto, N. Nakashima, K. Yoshihara, *Bull. Chem. Soc. Jpn.* 56 (1983) 3588–3594.
- [22] C. Schwer, M.G. Kenndler, *Anal. Chem.* 63 (1991) 1801–1807.
- [23] S.R. Shaota, M.G. Khaledi, *Anal. Chem.* 66 (1994) 1141–1146.
- [24] T. Yashima, A. Tsuchiya, O. Morita, S. Terabe, *Anal. Chem.* 64 (1992) 2981–2984.
- [25] S. Fujiwara, S. Honda, *Anal. Chem.* 59 (1987) 487–490.
- [26] J. Flanagan Jr., B. Legendre Jr., R. Hammer, S. Soper, *Anal. Chem.* 67 (1995) 341–347.
- [27] D. Chen, N.J. Dovichi, *Anal. Chem.* 68 (1996) 690–696.
- [28] C. Schwer, E. Kenndler, *Anal. Chem.* 63 (1991) 1801–1807.